Food Research 8 (Suppl. 1) : 125 - 135 (2024)
Journal homepage: https://www.myfoodresearch.com

FOOD RESEARCH

RESEARCH PAPER

The optimization of paddy drying in the rotary dryer: energy efficiency and product quality aspects analysis

[1]A'yuni, D.Q., [2]Subagio, A., [1]Prasetyaningrum, A., [1]Sasongko, S.B. and [1,*]Djaeni, M.

[1]*Department of Chemical Engineering, Faculty of Engineering, Diponegoro University Semarang, Indonesia*
[2]*Department of Physic Faculty of Science and Mathematics Diponegoro University, Semarang, Indonesia*

Article history:
Received: 7 March 2023
Received in revised form: 31 October 2023
Accepted: 17 December 2023
Available Online: 3 March 2024

Keywords:
Rotary dryer,
Paddy quality,
Energy efficiency,
RSM

DOI:
https://doi.org/10.26656/fr.2017.8(S1).17

Abstract

Currently, paddy drying has been widely developed and applied. This research goal was to find the optimal condition of paddy dried in a rotary dryer. The process was conducted at various paddy capacities (10–40 kg) and temperatures (40–60°C). For main indicators, the drying time, physical quality of the product and energy efficiency were evaluated. In doing so, the optimization process with the response surface method (RSM) was conducted. Results showed that under higher temperatures, the moisture level in the paddy reduced quickly, resulting in a shorter drying time and higher efficiency. However, faster moisture reduction can break the texture of paddy, which increases the percentage of broken rice. Meanwhile, with the increasing paddy capacity, heat transfer becomes more effective, as seen in the increase in energy efficiency. Nevertheless, the excessive capacity requires a longer drying time. After optimizing by response surface method (RSM), the most favorable condition can be reached at paddy capacity of 45.8 kg with drying temperature of 56.4°C. For this condition, energy efficiency achieved 15.6% with percentage of broken rice 8.18%.

1. Introduction

Rice (*Oryza sativa* L.) is an important crop that is widely consumed around the world. In 2020, the paddy production in Asia was approximately 680 million tons, resulting in around 450 million tons of rice (Food Agriculture Organization of the United Nations, 2022). The freshly harvested paddy mostly contains 20–27% w.b. moisture content, different for each season (Yahya *et al*., 2017; Yahya *et al*., 2018). Therefore, for prolonging storage life, the moisture content must be reduced to 14–15% to keep the quality before being saved and consumed (Badan Standarisasi Nasional, 2015).

One of the most popular methods for reducing the moisture content of freshly harvested paddy is direct sun drying. However, this method is weather dependency on both paddy quality and continuity. As an example, rice drying using a solar bubble dryer (SBD) needed approximately 18 hours (Aktar, 2022). Another method (convective dryer) obtained dry paddy grains after 20- and 30-minutes process at 80 and 70°C, respectively (Golpour, 2021). Meanwhile, a different study observed the application of a microwave oven for the paddy drying process that took 20 mins at a power of 22.99 W/g (Silva *et al*., 2021). Long drying times, high temperatures, and high microwave power eventually resulted in physical damage to the paddy grains. The physical damage, such as rice breakage and the burned surface, was probably caused by the spontaneous evaporation.

As an energy-intensive process, energy aspects of paddy drying such as energy efficiency are important observations. For paddy drying with a fluidized bed operated at 70°C and 2.3 m/s air velocity, the heat consumption requires 20 MJ per kg of water evaporated (Khanali *et al*., 2016). Theoretically, it implies that the heat efficiency was around 12%. The study reported that in the case of rough paddy drying, the temperature had a more significant impact on the drying rate than the air velocity. Using a vertical screw conveyor dryer (VCSD) at the same temperature, the heat efficiency can be two-fold (Utari *et al*., 2022). Considering the energy input from the motor and blower or another supply in the drying system, the heat efficiency will be lower than the total energy efficiency. Tohidi *et al*. (2017) achieved energy efficiency in the range of 16–23% when applying a fixed deep bed dryer to the paddy grains at 50 to 60°C.

*Corresponding author.
Email: *moh.djaeni@live.undip.ac.id*

eISSN: 2550-2166
Published by Rynnye Lyan Resources

A process used a fixed bed and rotary dryer to process 3 tons of paddy with multilayer observation (Gazor and Alizadeh, 2020). The result showed that the moisture content between the top, middle, and low layers was not uniform, which led to an increasing percentage of broken rice. In contrast, drying using a rotary dryer produced a uniform moisture content and lower rice breakage. A rotary dryer agitated and mixed the product in a circulated drying column, resulting in homogeneous moisture content and physical quality (Firouzi *et al*., 2017). This uniform moisture content is produced by homogenous heat distribution that lower the heat loss in the process (Alit and Susana, 2022). Although several studies have reported the effect of rotary drying on paddy physical quality and energy consumption (Firouzi *et al*., 2017; Gazor and Alizadeh, 2020; Singh *et al*., 2022), the application of rotary dryer for large-scale application cannot be straightforward. It still needs to study the effect of important inputs such as temperature and capacity on energy efficiency and paddy quality. Therefore, this research discusses the effect of air temperature and paddy capacity on drying time, percentage of broken rice, and energy efficiency. To support the study, optimization with Response Surface Methodology (RSM) was applied. The results were also compared with the other paddy drying methods.

2. Materials and methods

2.1 Materials

Paddy was freshly harvested in October 2021 in Mijen, Semarang, Central Java with a diameter of 0.200±0.005 cm and length of 1.03±0.05 cm. Paddy grains were cleaned and moisturized to homogenize the initial water content of samples. The total moisture content of paddy grains was measured for every run with an average value of 24.04±0.40% wet basis.

2.2 Drying experiment

Samples were dried using a rotary dryer with a column dimension of 0.75×1.2 m. The dryer setup consists of a blower, a heat source, a temperature controller, and a drying column that is equipped with a door for the final product. In this experiment, the rotation speed of the drying chamber is 6 rpm. As a drying medium, the ambient air with a linear velocity of 9.5 m/s was heated by liquid petroleum gas (LPG) combustion up to the desired drying temperature.

The paddy drying was operated at temperatures of 40, 50 and 60°C for 3 hrs with different capacities (10, 20, 30 and 40 kg). For an indicator, the moisture content of paddy was measured every 30 mins using a G-WON 87 GMK 303RS grain moisture meter (accuracy of 0.5% and 0.1% resolution).

2.3 Rice grading

The physical quality of the rice was observed after drying. The process includes paddy milling, followed by the separation of husk and rice. A laboratory-scale machine model 3 in 1 type IR-3 number 122002 (CV. Bumi Makmur Sadayana, Indonesia) milled 50 g of paddy samples. The machine was equipped with a blower to separate the husk from the rice. After that, a mini rice grader (BIMAPRO lab grader with serial number 11/BMA/2019) was used for classifying the percentage of head and broken rice.

2.4 Energy efficiency

This experiment estimated the energy efficiency at several drying temperatures and capacities. The energy efficiency was calculated using the equation:

$$\eta = \frac{X_p \lambda}{Q + P_b + P_m} \quad (1)$$

where X_p is the mass of evaporated water (kg), λ is the latent heat of vaporization (2400 kJ/kg), Q is the heat consumed (kJ), P_b and P_m are the power of the blower and motor (kJ).

2.5 Drying models

The mathematical model for the drying process was described by several models, as listed in Table 1. The moisture ratio from model was fitted with the experiment result to find the most suitable models. Moisture ratio (*MR*) from the experiment was expressed as follows:

$$MR = \frac{(M_t - M_e)}{(M_o - M_e)} \quad (2)$$

where M_t, M_o, M_e were moisture content of paddy at sampling time, initial, and equilibrium (% dry basis), respectively. The equilibrium moisture content was calculated using GAB equation as

$$M_e = \frac{abH_R(c/T)}{(1 - bH_R)(1 - bH_R + (c/T)bH_R)} \quad (3)$$

where HR was relative humidity and T was the drying temperature (°C). The GAB constants expressed in *a*, *b* and *c*, are cited from the previous result (Djaeni *et al*., 2013). Drying constants from every model were applied to predict drying time at different temperatures and capacity to dry paddy grains until 14% (w.b.). Validation of models used statistical parameters including coefficient correlation (R^2) and sum of square error (SSE).

2.6 Response surface methodology

The experiment was designed using Central Composite Design (CCD) to conduct experiments to find the optimum process of paddy drying in terms of

https://doi.org/10.26656/fr.2017.8(S1).17

Table 1. Mathematical models for the drying process.

Model	Equation	References
Newton	$MR = exp(-kt)$	(Ertekin and Firat, 2017)
Page	$MR = exp(-kt^n)$	(Oforkansi and Odoula, 2016)
Henderson and Pabis	$MR = a \cdot \exp(-kt)$	(Jian and Jayas, 2018)
Wang and Singh	$MR = 1 + at + bt^2$	(Ertekin and Firat, 2017)
Modified Page	$MR = exp(-kt)^n$	(Oforkansi and Odoula, 2016)
Logarithmic	$MR = a \cdot \exp(-kt) + c$	(Ertekin and Firat, 2017)

physical quality and energy efficiency. The design consisted of 13 runs with drying temperature (X_1) and capacity (X_2) as variables. The CCD and factor levels are depicted in Table 2.

3. Results and discussion

3.1 Observation of paddy moisture content

Figure 1 shows that the capacity affected the moisture content removal. Increasing the paddy capacity prolonged the drying process because of a higher load of moisture content. As can be seen at every temperature, the moisture content at the capacity of 40 kg was the highest. This result follows previous research that produced dry paddy grains longer at a higher capacity (Sitorus *et al*., 2021). It is also represented that at 60°C the drying rate was higher at the initial period than the latter (after 90 mins). This phenomenon followed the theory that freshly harvested paddy still has high free moisture on its surface, causing an easy moisture transfer to the air (Mondal *et al*., 2019). Afterward, additional heat is still required to completely evaporate bound moisture in the paddy.

Meanwhile, at all capacity for drying temperature of 40°C, the paddy cannot be fully dried (Figure 2-part (a)). Firouzi *et al*. (2017) found a similar result in the industrial rotary dryer with 3 tons of paddy grains loaded. After the dryer operated at 38 – 40°C with airflow of 0.015 $m^3m^{-2}s^{-1}$, it needs a long operational time (46 hours). Additionally, 250 g of rough rice was still in a wet condition after being processed under a digital forced air convection oven at 40°C for 6 hrs (Sadaka, 2022).

The target moisture content for paddy (14% w.b.) was aimed to produce dry grains that could be stored and milled properly. At the higher operational temperature, the paddy can be dried faster than that of the lower drying temperatures. For example, at 60°C and 20 kg, the drying time can be reduced to 90 mins (Figure 1). This experiment saved 2- and 6-hours drying time than process by vertical screw conveyor and air inflated solar dryer, respectively (Dubey, 2019; Utari *et al*., 2022). However, in the case of the application, a drying capacity of 40 kg seemed more profitable due to a much larger mass of paddy grains with a three-hour process.

Table 2. Central composite design with 3 levels and 2 variables for paddy drying using rotary dryer.

Run Order	Coded factor levels	
	Temperature	Capacity
1	-1.4142	0
2	1	-1
3	0	1.4142
4	0	0
5	0	0
6	0	0
7	-1	1
8	0	-1.4142
9	1.4142	0
10	0	0
11	1	1
12	-1	-1
13	0	0

Factors and levels for experimental design using CCD					
Variables	-α	-1	0	1	+α
Temperature (˚C)	35.86	40	50	60	64.14
Capacity (kg)	3.79	10	25	40	46.21

https://doi.org/10.26656/fr.2017.8(S1).17

Figure 1 also shows that the drying temperature had a significant moisture content, displayed in the high difference in final moisture content.

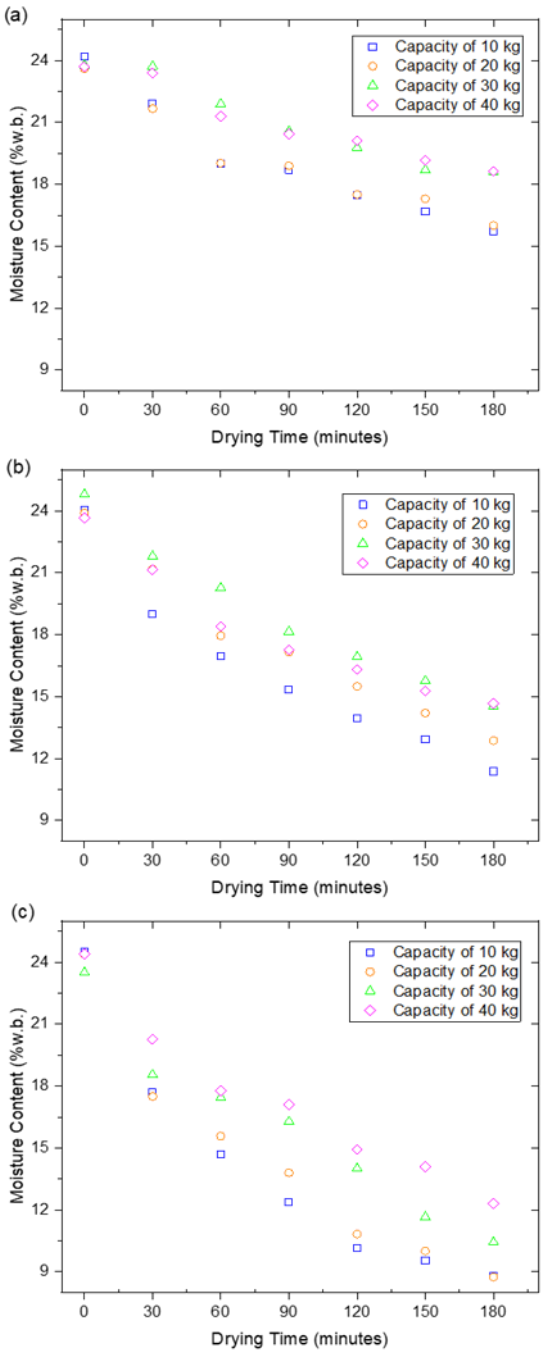

Figure 1. Moisture content of paddy through the drying process at temperature of (a) 40, (b) 50, and (c) 60˚C.

Based on the moisture removal and drying time, low capacity and high temperature had a better performance. Also, when the drying capacity increased, the drying speed, uniformity, and whiteness of paddy were reduced (Gu *et al*., 2022). Nevertheless, the ideal capacity must be found to minimize energy consumption or find the optimal process (Chen *et al*., 2020).

3.2 Physical quality of rice

An important physical quality of rice is the amount of broken rice. The physical quality of rice after a 3-hour drying process was shown in Table 3. Comparing the experimental results with the national standard of rice declared in Indonesian National Standard SNI 6128:2015 (2015), some of the results cannot be classified as standard-qualified rice. To achieve the minimum quality of the national standard, the rice has to have a maximum of 14 or 15% (w.b.) of moisture content with a maximum of 35% broken rice. The low-quality rice was found at 40 and 60°C. At temperatures of 40°C, the paddy did not achieve the standard because of its higher moisture content. Meanwhile, at a drying temperature of 60°C for 3 hrs, the moisture reduction was fast, which deteriorated the paddy texture as seen in the higher broken rice. Based on the national standard, the minimum quality of premium rice is supposed to be 14% moisture content and 5% broken rice. Therefore, from all of the processes, the best rice obtained was only of medium quality. The best possible choice to operate the dryer with high paddy quality is a drying capacity of 40 kg and a temperature of 60°C.

Based on the data in Table 3, the relationship between moisture content and broken rice is complicated. With a higher moisture content, the percentage of broken rice can be reduced. However, too high moisture content cannot fulfill the standard. A similar result had been discussed in previous research, whereby, even at the same moisture content, the total of unbroken rice can be different after being processed with different variables (Rahimi-Ajdadi *et al*., 2018). They found that almost every interaction of paddy variety, drying temperature, time, and moisture content had a significant effect on the unbroken rice. Overall, even with different types of dryers, the relationship between broken rice and moisture content was similar to this work (Jafari *et al*., 2017; Mondal *et al*., 2019). According to a previous experiment, the application of a high-energy microwave produced a lower moisture content and increased the grain's breakage (Jafari, 2017). A contrasting result was found by another study that also used a rotary dryer (Firouzi *et al*., 2017). They reported that paddy with low moisture content has high mechanical strength, so it has less broken rice.

3.3 Energy efficiency

Figure 2 shows the changes in energy efficiency over the drying time at capacities of 10 to 40 kg. The highest value was found at the operational temperature of 60°C with 40 kg capacity (32%), while the lowest was at 40°C and 10 kg (5%). These energy efficiencies are comparable with paddy drying results reported by Utari *et al*. (2022) for vertical screw conveyor dryer (20.27–26.31%), Yahya *et al*. (2018) for solar-assisted heat pump fluidized bed dryer integrated with biomass furnace (8.4–25.6%), and Tohidi *et al*. (2017) for fixed

https://doi.org/10.26656/fr.2017.8(S1).17

Table 3. Physical qualities of rice after three hours drying process and the classification based on SNI 6128:2015.

Temperature (˚C)	Capacity (kg)	Final Moisture Content (% w.b.)	Broken Rice (%)	Classification
40	10	15.73*	15.75	*Under standard
	20	16.00*	10	*Under standard
	30	18.60*	9.57	*Under standard
	40	18.63*	7.08	*Under standard
50	10	11.38	19.78	Medium 1
	20	12.88	16.49	Medium 1
	30	14.52	10.26	Medium 3
	40	14.67	10.35	Medium 3
60	10	8.8	66.45**	**Under standard
	20	8.77	62.50**	**Under standard
	30	10.42	19.85	Medium 1
	40	12.3	14.61	Medium 1

*Under standard due to the moisture content
**Under standard due to the broken rice

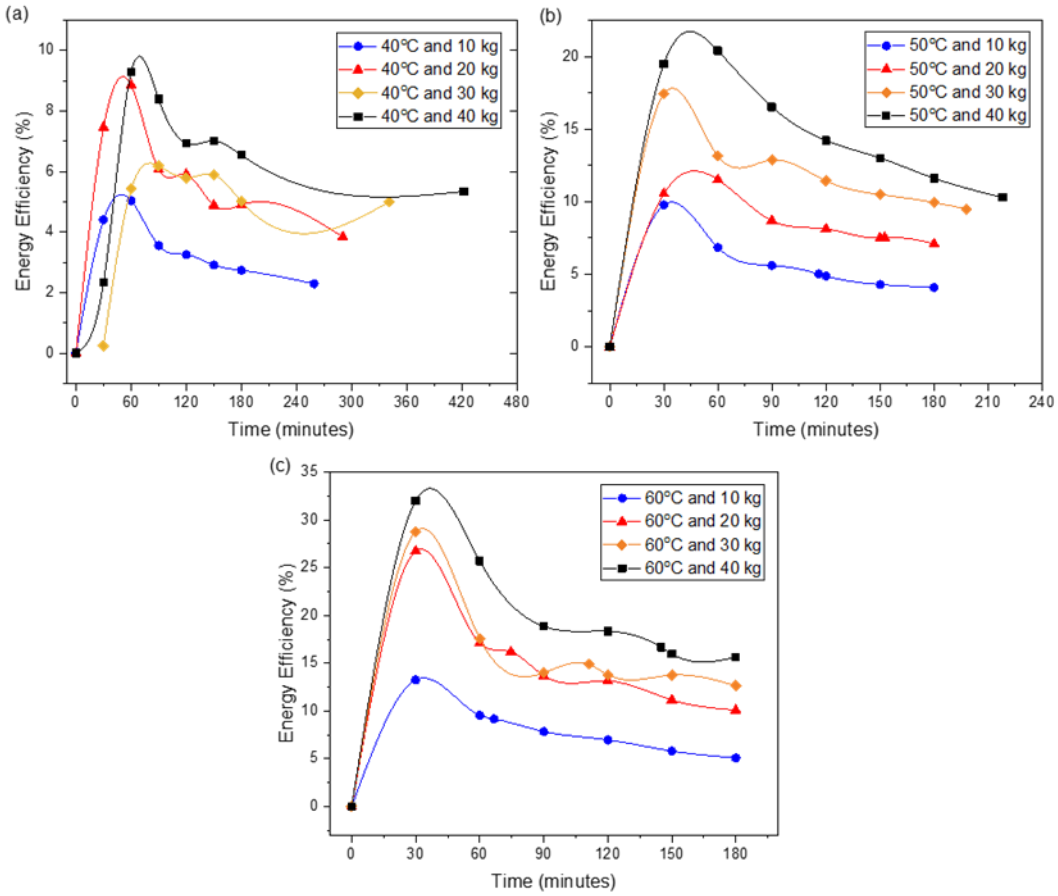

Figure 2. Variation of energy efficiency versus drying time at different temperatures and capacities.

bed dryer (5.57–33.93%).

This study's energy efficiency stages (Figure 2) correspond to the three drying stages identified in other studies: maximum efficiency, falling period, and constant period (Jafari, 2017). In the first stage, the efficiency reached its maximum value because of the high utilization of energy to evaporate the free moisture content on the paddy surface. Next, the value fell due to hardly vaporizing bound moisture inside paddy pores. At this point, the heat was only served to warm the solid product (de Brito, 2017). Energy efficiency eventually approached a near-steady state.

Table 4 show the result of the energy efficiency calculation based on equation 1. In this experiment, increasing the drying capacity at every temperature tent to increase energy efficiency. Proportionally, a higher operational temperature produced a more efficient drying process in terms of energy. A similar relationship between energy efficiency and temperature was also found by Hssaini *et al*. (2021) when figs were dried using a solar convective dryer. A contrasting result was obtained from an experiment, stating that the thermal

https://doi.org/10.26656/fr.2017.8(S1).17

efficiency was lower at high temperatures due to heat loss, causing high energy consumption (Rabha, 2017). Because of the impact of the drying temperature and capacity interaction (the significance of which can be seen in the RSM analysis), capacity must be considered in addition to temperature. For instance, even at a higher temperature, the energy efficiency at 60°C and 10 kg was lower than at a temperature of 50°C and capacity of 30 and 40 kg. That indicates heat loss from the dryer as well as a low load of water evaporating. Whereas much heat was required to reach drying temperature carried in sensible heat of air. Thus, to minimize heat loss, increasing the temperature can be done along with increasing the drying capacity.

Table 4. Energy efficiency of the three-hour drying process.

Temperature (˚C)	Capacity (kg)	Energy efficiency
40	10	2.3%
	20	3.8%
	30	5.0%
	40	5.3%
50	10	5.0%
	20	7.5%
	30	9.5%
	40	10.3%
60	10	9.2%
	20	16.2%
	30	14.9%
	40	16.7%

The additional load on the dryer made a greater water removal and resulted in better energy utilization. This result indicated that the maximum energy efficiency was found at the capacity of 40 kg at all temperatures. Nevertheless, a previous observation reported that increasing the temperature did not always have a significant effect on efficiency (de Brito *et al*., 2017). The report mentioned that increasing the thermal energy increased the temperature gradient between the drying column and the air and caused heat loss. One factor that also influences the energy usage of the drying process is the initial moisture content of paddy grains. For example, feeding paddy with a higher initial moisture content at the same temperature and airflow on the continuous crossflow dryer decreases the energy consumption of the process because of the ease of evaporating the wet surface (Hemhirun and Bunyawanichakul, 2020).

3.4 Drying models

All the drying models were fitted to the experimental data from different drying temperatures and capacities. Table 5 displays the model coefficient and statistical parameters in the form of coefficient correlation (R^2) and SSE. Every model shows good regressions that are indicated by R^2 close to 1 and SSE close to 0 of all conditions. The lowest R^2 value was found at temperature of 40°C and capacity of 20 kg at the Henderson and Pabis model (0.938), while most of the highest values of R^2 were obtained by the Page models. Apart from that, drying 40 kg of paddy at temperatures of 40 and 50°C fits the Newton and Logarithmic model, respectively. The three models show good fit with R^2 close to 1 and SSE close to 0. According to the most suitable models, a comparison of experimental and predicted values was exhibited in Figure 3. Jafari *et al*. (2017) and Dubey *et al*. (2019) also found Page model as the most suitable model to estimate the drying rate of paddy drying using microwave and solar drying, respectively. A different study obtained Midili as the best model after drying paddy grains in the fluidized bed dryer (Sitorus *et al*., 2021). The differences in which model was found to be the most suitable were based on drying process factors and variables such as paddy initial moisture content, drying temperature, and capacity (Sitorus *et al*., 2021).

Figure 3 shows the predicted drying times from initial moisture content to 14% w.b. at different temperatures and capacities using the most suitable models. Based on the graph, increasing the drying temperature had given a significant impact on the drying time. From the bar, there are far distances between drying time at 40°C and two other temperatures. With only a 10°C temperature difference, the drying time can be reduced by more than 100%. For comparison, two cases of paddy drying at different temperatures had been conducted by Mondal *et al*. (2019) and Hemhirun and Bunyawanichakul (2020) using a flow dryer. At a much higher temperature, 150°C, the dried samples can be obtained in less than one hour, while at 45°C operations, they can be reached after almost three hours of the drying process. This significant result was also found when the temperature increased from 50 to 60°C (Figure 4). Loading a higher capacity on the drying column had a significant impact on the drying time similar as the temperatures. As clearly seen in the graph, increasing 10 kg of body mass on the column made a longer drying time.

3.5 Response surface methodology

This research aimed to produce dry paddy grains (14% w.b.) with low broken rice and high efficiency. The polynomial equations to find these responses were estimated based on Central Composite Design (CCD) in Table 2. According to the experimental design, the empirical relationship between responses and factors in the coded units was expressed as

$$Moisture\ Content = 13.70 - 3.19X_1 + 2.01X_2 - 0.141{X_1}^2 - 0.249{X_2}^2 + 0.148X_1X_2 \quad (4)$$

$$Broken\ Rice = 14.90 + 14.24X_1 - 9.64X_2 + 7.27{X_1}^2 + 2.14{X_2}^2 - 10.80X_1X_2 \quad (5)$$

https://doi.org/10.26656/fr.2017.8(S1).17

Table 5. Model coefficients and R^2 of several drying models at different drying conditions.

Model	Temperature (°C)	Model Coefficient			
		Capacity 10 kg	Capacity 20 kg	Capacity 30 kg	Capacity 40 kg
Newton	40	k = 0.0039 R^2 = 0.9534 SSE = 0.0230	k = 0.0039 R^2 = 0.9505 SSE = 0.0116	k = 0.0029 R^2 = 0.9608* SSE = 0.0078	k = 0.0027 R^2 = 0.9605* SSE = 0.0052
	50	k = 0.0065 R^2 = 0.9615 SSE = 0.0216	k = 0.0053 R^2 = 0.9836 SSE = 0.0060	k = 0.0049 R^2 = 0.9914 SSE = 0.0036	k = 0.0048 R^2 = 0.9724 SSE = 0.0084
	60	k = 0.0087 R^2 = 0.9563 SSE = 0.0323	k = 0.0082 R^2 = 0.9589 SSE = 0.0274	k = 0.0065 R^2 = 0.9662 SSE = 0.0144	k = 0.0056 R^2 = 0.9692 SSE = 0.0137
Henderson and Pabis	40	a = 0.9607 k = 0.0042 R^2 = 0.9467 SSE = 0.0091	a = 0.9635 k = 0.0037 R^2 = 0.9384 SSE = 0.0089	a = 1.0308 k = 0.0031 R^2 = 0.9532 SSE = 0.0061	a = 1.0082 k = 0.0028 R^2 = 0.9529 SSE = 0.0050
	50	a = 0.9346 k = 0.0063 R^2 = 0.9508 SSE = 0.0127	a = 0.9749 k = 0.0052 R^2 = 0.9796 SSE = 0.0046	a = 0.9739 k = 0.0048 R^2 = 0.9891 SSE = 0.0022	a = 0.9652 k = 0.0046 R^2 = 0.9652 SSE = 0.0067
	60	a = 0.9351 k = 0.0091 R^2 = 0.9480 SSE = 0.0183	a = 0.9325 k = 0.0082 R^2 = 0.9489 SSE = 0.0169	a = 0.9553 k = 0.0062 R^2 =0.9590 SSE = 0.0113	a = 0.9491 k = 0.0054 R^2 = 0.9610 SSE = 0.0088
Page	40	n = 0.7188 k = 0.0176 R^2 = 0.9785* SSE = 0.0037	n = 0.7187 k = 0.0155 R^2 = 0.9696* SSE = 0.0044	n = 1.1739 k = 0.0012 R^2 = 0.9506 SSE = 0.0064	n = 0.9901 k = 0.0029 R^2 = 0.9518 SSE = 0.0052
	50	n = 0.6497 k = 0.0363 R^2 = 0.9974* SSE = 6.769×10^{-4}	n = 0.8265 k = 0.0124 R^2 = 0.9902* SSE = 0.0022	n = 0.8311 k = 0.0112 R^2 = 0.9976* SSE = 4.919×10^{-4}	n = 0.7522 k = 0.0162 R^2 = 0.9899 SSE = 0.0019
	60	n = 0.6477 k = 0.0497 R^2 = 0.9974* SSE = 9.188×10^{-4}	n = 0.6581 k = 0.0438 R^2 = 0.9907* SSE = 0.0031	n = 0.7878 k = 0.0181 R^2 = 0.9679* SSE = 0.0088	n = 0.7077 k = 0.0235 R^2 = 0.9902* SSE = 0.0022
Wang and Singh	40	a = -0.0055 b = 1.5070×10^{-5} R^2 = 0.9713 SSE = 0.0049	a = -0.0049 b = 1.2969×10^{-5} R^2 = 0.9618 SSE = 0.0055	a = -0.0026 b = 1.9925×10^{-6} R^2 = 0.9428 SSE = 0.0074	a = -0.0029 b = 4.5177×10^{-6} R^2 = 0.9547 SSE = 0.0048
	50	a = -0.00765 b = 2.2873×10^{-5} R^2 = 0.9545 SSE = 0.0118	a = -0.00577 b = 1.4110×10^{-5} R^2 = 0.9843 SSE = 0.0035	a = -0.00537 b = 1.2530×10^{-5} R^2 = 0.9921 SSE = 0.0016	a = -0.00581 b = 1.5929×10^{-5} R^2 = 0.9892 SSE = 0.0021
	60	a = -0.0100 b = 3.3708×10^{-5} R^2 = 0.9669 SSE = 0.0117	a = -0.0090 b = 2.8168×10^{-5} R^2 = 0.9436 SSE = 0.0187	a = -0.0064 b = 1.4870×10^{-5} R^2 = 0.9423 SSE = 0.0159	a = -0.0064 b = 1.7407×10^{-5} R^2 = 0.9607 SSE = 0.0088
Modified Page	40	a = 1.0042 n = 0.7115 k = 0.0036 R^2 = 0.9733 SSE = 0.0036	a = 1.0039 n = 0.7111 k = 0.0030 R^2 = 0.9622 SSE = 0.0044	a = 1.0222 n = 1.0878 k = 0.0033 R^2 = 0.9442 SSE = 0.0058	a = 1.0142 n = 0.9402 k = 0.0027 R^2 = 0.9425 SSE = 0.0049
	50	a = 0.9982 n = 0.6520 k = 0.0061 R^2 = 0.9967 SSE = 6.737×10^{-4}	a = 1.0028 n = 0.8214 k = 0.0049 R^2 = 0.9877 SSE = 0.0022	a = 0.9986 n = 0.8340 k = 0.0045 R^2 = 0.9970 SSE = 4.901×10^{-4}	a = 1.0048 n = 0.7439 k = 0.0042 R^2 = 0.9876 SSE = 0.0019
	60	a = 1.0008 n = 0.6468 k = 0.0097 R^2 = 0.9967 SSE = 9.181×10^{-4}	a = 0.9967 n = 0.6617 k = 0.0086 R^2 = 0.9884 SSE = 0.0031	a = 0.9876 n = 0.8110 k = 0.0061 R^2 = 0.9605 SSE = 0.0087	a = 0.9978 n = 0.7113 k = 0.0050 R^2 = 0.9879 SSE = 0.0022

*The highest R^2 at every temperature and capacity.

https://doi.org/10.26656/fr.2017.8(S1).17

Table 5 (Cont.). Model coefficients and R^2 of several drying models at different drying conditions.

Model	Temperature (°C)	Model Coefficient			
		Capacity 10 kg	Capacity 20 kg	Capacity 30 kg	Capacity 40 kg
Logarithmic	40	a = 0.5805 k = 0.0115 C = 0.4205 R^2 = 0.9761 SSE = 0.0033	a = 0.5415 k = 0.0108 C = 0.4592 R^2 = 0.9642 SSE = 0.0041	a = 0.9408 k = 0.0035 C = 0.0920 R^2 = 0.9417 SSE = 0.0061	a = 0.6413 k = 0.0054 C = 0.3787 R^2 = 0.9479 SSE = 0.0044
	50	a = 0.6766 k = 0.0142 C = 0.3062 R^2 = 0.9808 SSE = 0.0040	a = 0.7292 k = 0.0090 C = 0.2690 R^2 = 0.9870 SSE = 0.0023	a = 0.7361 k = 0.0078 C = 0.2560 R^2 = 0.9948 SSE = 8.414×10^{-4}	a = 0.6257 k = 0.0111 C = 0.3772 R^2 = 0.9928* SSE = 0.0011
	60	a = 0.7572 k = 0.0184 C = 0.2340 R^2 = 0.9937 SSE = 0.0018	a = 0.7504 k = 0.0154 C = 0.2269 R^2 = 0.9698 SSE = 0.0080	a = 0.8826 k = 0.0072 C = 0.0790 R^2 = 0.9495 SSE = 0.0111	a = 0.6733 k = 0.0110 C = 0.3102 R^2 = 0.9750 SSE = 0.0045

*The highest R^2 at every temperature and capacity.

$$Energy\ Efficiency = 7.65 + 3.06\,X_1 + 3.21X_2 - 0.45{X_1}^2 + 0.04{X_2}^2 + 1.87X_1X_2 \quad (6)$$

Based on ANOVA (Table 6), the effect of temperature and capacity is significant to moisture content, broken rice, and energy efficiency (p-value <0.05). Based on equations (4) to (6), the proportional relationship between drying temperature and response is found at broken rice and energy efficiency. This implies that raising the drying temperature will result in less moisture content and more broken rice and higher efficiency. The interaction of two factors (temperature and capacity) affects the broken rice and energy efficiency significantly. ANOVA shows a fit of the models on the drying experiment with R^2 close to 1.

The polynomial equations were then used to make a three-dimensional plot of four responses at different drying temperatures and capacities (Figure 5). Different relationships were observed in every response. From Figure 5 (a), the relationship between moisture content and drying temperature is different from capacity. Therefore, the lowest moisture content is found at the highest temperature and lowest capacity. It is also demonstrated that the lowest broken rice is at low temperature and high capacity, particularly when processed below 45°C. At a high temperature and low capacity, the paddy was highly exposed to heat, which led to sample breakage. In another response, the lowest value of energy efficiency is at the lowest capacity and the highest temperature. Hence, the optimum response was estimated to find suitable factors in the drying process. From the statistical analysis using RSM, Table 7 displayed the optimization of the response. The estimation shows that dry paddy with 8.18% broken rice and 15.64% energy efficiency can be reached at a drying temperature of 56.4°C and capacity of 45.8 kg. The composite desirability was close to 1, indicating a suitable optimization to reach the goal.

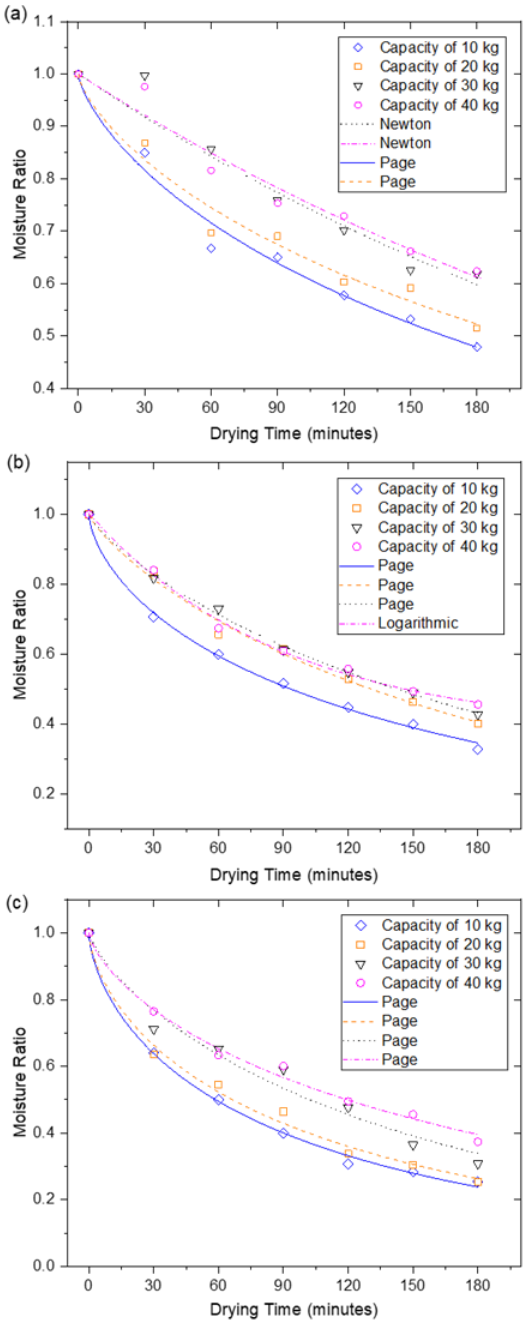

Figure 3. Moisture removal based on drying models at (a) 40 (b) 50 (c) 60°C.

https://doi.org/10.26656/fr.2017.8(S1).17

Table 6. ANOVA of two factors on the responses.

Source	P-value		
	Moisture Content	Broken Rice	Energy Efficiency
Linear			
X_1	0.001*	0.001*	0.001*
X_2	0.001*	0.003*	0.001*
Square			
X_1^2	0.648	0.018*	0.113
X_2^2	0.428	0.398	0.866
2-Way Interaction			
$X_1 X_2$	0.716	0.011*	0.001*
R^2 (adj)	0.938	0.865	0.970

*Significant at 5%

Table 7. Response optimization of paddy drying using rotary dryer for three hours.

Drying Temperature (˚C)	Capacity (kg)	Energy Efficiency (%)	Moisture Content (% w.b.)	Broken Rice (%)	Composite Desirability
56.43	45.78	15.64	14.03	8.18	0.9919

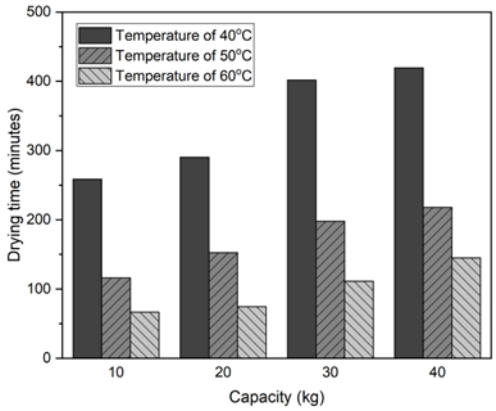

Figure 4. The predicted drying time at different drying temperature and capacity based on the drying models.

4. Conclusion

This research observed the effects of drying temperature and capacity on paddy drying using a rotary dryer, including moisture removal, physical quality, and energy efficiency. The fastest drying time was found to be at 60°C and capacity of 10 kg, with a process that took less than 90 minutes to produce dry paddy with a moisture content of 14% w.b. According to the national standard, the highest quality grains (Medium I) are found after being processed at temperatures of 50 and 60°C at capacity 10 – 20 kg and 30 – 40 kg, respectively. Overall, increasing the capacity and temperature had an impact on increasing energy efficiency. Based on the drying models, the Page, Newton, and Logarithmic models showed the best fit to the experiments and to predict the drying time at every temperature and capacity. Using RSM, the best conditions for paddy drying in this rotary dryer were at temperature 56.4°C and capacity of 45.8 kg with energy efficiency of 15.64% and percentage of broken rice of 8.18%.

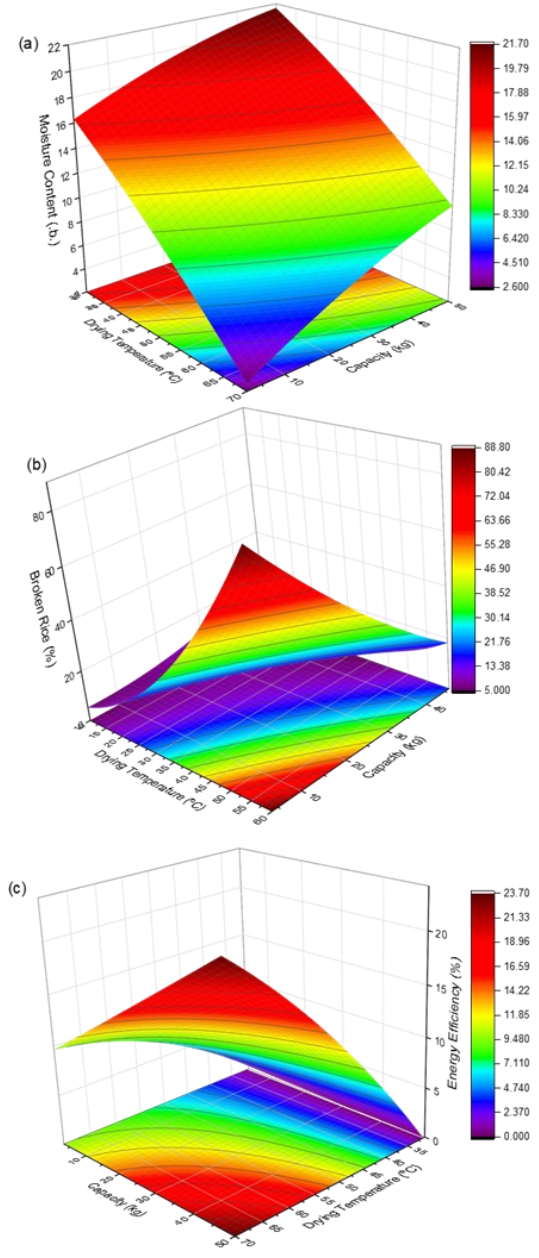

Figure 5. Three-dimensional plot of (a) moisture content, (b) broken rice, and (c) energy efficiency of two factors.

https://doi.org/10.26656/fr.2017.8(S1).17

Conflict of interest

The authors declare no conflict of interest.

Acknowledgments

This research was funded by DRTPM DIKTI Kemendikbud Indonesia.

References

Aktar, S., Alam, M.A., Saha, C.K. and Roy, J.C. (2022). Solar bubble dryer: Alternative to sun drying for reducing drying losses. *Bangladesh Journal of Agriculture*, 47(1), 60589. https://doi.org/10.3329/bjagri.v47i1.60589

Alit, I.B. and Susana I.G.B. (2022). Rotary dryer in a study based on participatory principles for smallholder scale drying. *Global Journal of Engineering and Technology Advances*, 12(2), 72-77. https://doi.org/10.30574/gjeta.2022.12.2.0139

Badan Standarisasi Nasional. (2015). Beras (SNI 6128:2015). Retrieved from SNI website: pbsn_4-2021_lampiran_xvii_skema_beras.pdf. [In Bahasa Indonesia].

Chen, C., Venkitasamy, C., Zhang, W., Deng, L., Meng, X. and Pan, Z. (2020). Effect of step-down temperature drying on energy consumption and product quality of walnuts. *Journal of Food Engineering*, 285, 110105. https://doi.org/10.1016/j.jfoodeng.2020.110105

de Brito, R.C., de Pádua, T.F., Freire, J.T. and Béttega, R. (2017). Effect of mechanical energy on the energy efficiency of spouted beds applied on drying of sorghum [*Sorghum bicolor* (L) moench]. *Chemical Engineering and Processing: Process Intensification*, 117, 95–105. https://doi.org/10.1016/j.cep.2017.03.021

Djaeni, M., Ayuningtyas, D., Asiah, N., Hargono, H., Ratnawati, R., Wiratno, W. and Jumali, J. (2013). Paddy drying in mixed adsorption dryer with zeolite: drying rate and time estimation. *Reaktor*, 14(3), 173. https://doi.org/10.14710/reaktor.14.3.173-178

Dubey, A., Sharma, P.K., Mani, I., Parray, R.A., Aradwad, P. and Tv, A.K. (2019). Mathematical modelling of drying kinetics of paddy in sun drying and air inflated solar dryer. *International Journal of Chemical Studies*, 7(1), 1122–1126.

Ertekin, C. and Firat, M.Z. (2017). A comprehensive review of thin-layer drying models used in agricultural products. *Critical Reviews on Food Science and Nutrition*, 57(4), 701–717. https://doi.org/10.1080/10408398.2014.910493

Firouzi, S., Alizadeh, M.R. and Haghtalab, D. (2017). Energy consumption and rice milling quality upon drying paddy with a newly-designed horizontal rotary dryer. *Energy*, 119, 629–636. https://doi.org/10.1016/j.energy.2016.11.026

Food Agriculture Organization of the United Nations. (2022). FAOStat Database. Retrieved on July 4, 2022 from FAO website: https://www.fao.org/faostat/en/#compare

Gazor, H.R. and Alizadeh, M.R. (2020). Comparison of rotary dryer with conventional fixed bed dryer for paddy drying, milling quality and energy consumption. *Agricultural Engineering International: CIGR Journal*, 22(2), 264–271.

Golpour, I., Pinho, R., Guine, F., Amiri, R. and Bu-Ali, C. (2021). Evaluating the heat and mass transfer effective coefficients during the convective drying process of paddy (*Oryza sativa* L.). *Journal of Food Process Engineering*, 44(9), e13771. https://doi.org/10.1111/jfpe.13771

Gu, X., Dai, J., Li, H. and Dai, Y. (2022). Experimental and theoretical assessment of a solar assisted heat pump system for in-bin grain drying: A comprehensive case study. *Renewable Energy*, 181, 426-444. https://doi.org/10.1016/j.renene.2021.09.049

Hemhirun, S. and Bunyawanichakul, P. (2020). Effect of the initial moisture content of the paddy drying operation for the small community. *Journal of Agricultural Engineering*, 51, 176–183. https://doi.org/10.4081/jae.2020.1079

Hssaini, L., Ouaabou, R., Hanine, H., Razouk, R. and Idlimam, A. (2021). Kinetics, energy efficiency and mathematical modeling of thin layer solar drying of figs (*Ficus carica* L.). *Science Reports*, 11, 21266. https://doi.org/10.1038/s41598-021-00690-z

Jafari, H., Kalantari, D. and Azadbakht, M. (2017). Semi-industrial continuous band microwave dryer for energy and exergy analyses, mathematical modeling of paddy drying and its qualitative study. *Energy*, 138, 1016–1029. https://doi.org/10.1016/j.energy.2017.07.111

Jian, F. and Jayas, D.S. (2018). Characterization of isotherms and thin-layer drying of red kidney beans, part i: Choosing appropriate empirical and semitheoretical models. *Drying Technology*, 36, 1696–1706. https://doi.org/10.1080/07373937.2017.1422515

Khanali, M., Banisharif, A. and Rafiee, S. (2016). Modeling of moisture diffusivity, activation energy and energy consumption in fluidized bed drying of rough rice. *Heat and Mass Transfer*, 52(11), 2541–2549. https://doi.org/10.1007/s00231-016-1763-z

Mondal, M.H.T., Shiplu, K.S.P., Sen, K.P., Roy, J. and Sarker, M.S.H. (2019). Performance evaluation of small scale energy efficient mixed flow dryer for drying of high moisture paddy. *Drying Technology*, 37(12), 1541–1550. https://doi.org/10.1080/07373937.2018.1518914

Oforkansi, B.C. and Odoula, M.K. (2016). Mathematical model of thin-layer drying process in a plantain sample. *International Journal of Engineering Research*, 5(5), 364–366.

Rabha, D.K., Muthukumar, P. and Somayaji, C. (2017). Energy and exergy analyses of the solar drying processes of ghost chilli pepper and ginger. *Renewable Energy*, 105, 764–773. https://doi.org/10.1016/j.renene.2017.01.007

Rahimi-Ajdadi, F., Asli-Ardeh, E.A. and Ahmadi-Ara, A. (2018). Effect of varying parboiling conditions on head rice yield for common paddy varieties in Iran. *Acta Technologica Agriculturae*, 21, 1–7. https://doi.org/10.2478/ata-2018-0001

Sadaka, S. (2022). Determination of short-grain rough rice drying kinetics under isothermal conditions using an integrated model. *Bioresources*, 17(3), 4001-4017. https://doi.org/10.15376/biores.17.3.4001-4017

Silva, E.G., Gomez, R.S., Gomes, J.P., Silva, W.P., Porto, K.Y.N., Rolim, F.D., Carmo, J.E.F., Andrade, R.O., Santos, I.B., Sousa, R.A.A., Diniz, D.D.S., Aragão, M.M.C.A. and Lima, A.G.B. (2021). Heat and mass transfer on the microwave drying of rough rice grains: An experimental analysis. *Agriculture*, 11(1), 8. https://doi.org/10.3390/agriculture11010008

Singh, P., Mahanta, P. and Kalita, P. Experimental investigation of paddy drying characteristics in a slitless rotary fluidized-bed dryer. *Drying Technology*, 40(15), 3262-3272. https://doi.org/10.1080/07373937.2021.2018700

Sitorus, A., Novrinaldi, Putra, S.A., Cebro, I.S. and Bulan, R. (2021). Modelling drying kinetics of paddy in swirling fluidized bed dryer. *Case Studies in Thermal Engineering*, 28, 101572. https://doi.org/10.1016/j.csite.2021.101572

Tohidi, M., Sadeghi, M. and Torki-Harchegani, M. (2017). Energy and quality aspects for fixed deep bed drying of paddy. *Renewable and Sustainable Energy Reviews*, 70, 519–528. https://doi.org/10.1016/j.rser.2016.11.196

Utari, F.D., Yasintasia, C., Ratridewi, M., A'yuni, D.Q., Kumoro, A.C., Djaeni, M. and Asiah, N. (2022). Evaluation of paddy drying with vertical screw conveyor dryer (VSCD) at different air velocities and temperatures. *Chemical Engineering and Processing: Process Intensification*, 174, 108881. https://doi.org/10.1016/j.cep.2022.108881

Yahya, M., Fudholi, A. and Sopian, K. (2017). Energy and exergy analyses of solar-assisted fluidized bed drying integrated with biomass furnace. *Renewable Energy*, 105, 22-29. https://doi.org/10.1016/j.renene.2016.12.049

Yahya, M., Fahmi, H., Fudholi, A. and Sopian K. (2018). Performance and economic analyses on solar-assisted heat pump fluidised bed dryer integrated with biomass furnace for rice drying. *Solar Energy*, 174, 1058-1067. https://doi.org/10.1016/j.solener.2018.10.002

https://doi.org/10.26656/fr.2017.8(S1).17